

## RESEARCH ARTICLE

Issue 5, May 2004

## Engineering &amp; Applied Sciences

## Photobleaching of cresyl violet in poly(methyl methacrylate)

**Michael J. Holmes, 2nd Lt., USMC**

Strike Training Squadron Nine, Naval Air Station, Meridian MS

**Advisor: Carl E. Mungan, Ph.D.**

U.S. Naval Academy

## Abstract

This study investigates the rapidity with which an optical dye in a solid plastic host irreversibly degrades when it is brightly illuminated by visible light. Specifically, the organic dye cresyl violet perchlorate dispersed in plexiglas was optically excited by a continuous-wave dye laser pumped by an argon-ion laser. After resonantly absorbing and emitting many times, an individual dye molecule photochemically bleaches. The decay of the overall fluorescence signal was measured and fit to a theoretical model describing the time dependence of the bleaching in terms of a quantum efficiency for photooxidation. Under ambient conditions, it takes a few million excitation-relaxation cycles to bleach a dye molecule at incident intensities on the order of 100 W/cm<sup>2</sup>. This permanently destroys the dye, thereby limiting applications of such organic materials under exposure to high optical intensities, in laser sensors or fibers, for example.

## Introduction

Laser dyes are organic compounds that relax radiatively after optical excitation, emitting in the visible or infrared range. The first laser dye, phthalocyanine, was discovered in 1966 by Sorokin and Lankard but is seldom employed in lasers today. Only a year later, rhodamine 6G (Rh6G) was discovered and continues to be the most widely used laser dye (Drexhage 1990). Today a large variety of luminescent dyes have been optimized for use in circulating liquid lasers.

These dyes have a range of practical applications when rigidized in a polymer host. One area that may be revolutionized by the use of organic luminophores in plastics is the flat-screen monitor industry. Current thin screens typically use expensive, delicate plasma technology. Organic emitters doped in a polymer layer offer an inexpensive, malleable, and easy-to-produce alternative. Organic dyes are also of interest for sensors, optical amplifiers, and fiber optics.

If organic fluorescent molecules are to be effectively used in such applications, they must be able to withstand repeated excitations and the large amounts of energy that will be cycled through them. Unfortunately, upon repeated absorption, the dye molecules begin to photooxidize, and they consequently lose the ability to fluoresce (Mackey 2001).

Cresyl violet (C<sub>16</sub>H<sub>12</sub>N<sub>3</sub>O<sub>5</sub>Cl), technically known as 5,9-diaminobenzo[a]phenoxazonium perchlorate (or oxazine 9 for short) and commonly referred to in the trade as LC6700 or CV670, is an efficient emitter at far red wavelengths (Castelli 1975). It is stable under ambient conditions, with minimal power saturation even at peak intensities as high as 100 MW/cm<sup>2</sup> (Moore 1978). It has a molecular weight of 361.74 g/mol, and its absorption spectrum is a good match to the emission from an Rh6G dye laser — the laser dye most widely used today.

Our experiment consisted of irradiating cresyl violet (CV) doped in thin solid slabs of poly(methyl methacrylate) with progressively higher intensities of Rh6G-laser light tuned to an absorption peak of the CV molecule. We expected the molecules would eventually photooxidize during this process of repeated excitation and relaxation of the electronic energy levels responsible for the violet color of the CV dye. This occurs because there is a weak but measurable probability that an excited molecule will make a transition into a chemically altered state as a result of a reaction with oxygen or water (originally dissolved in the dye and polymer solvents), rather than simply relaxing back to the ground state of the unreacted molecule (Schäfer 1992). By measuring the rate at which this occurs for different laser intensities, our goal was to quantify the quantum efficiency or probability for such a chemical transformation to occur. This can be accomplished by continuously monitoring the photoluminescence emitted by the relaxing CV molecules and fitting the decrease in this signal to a theoretical model describing the rate of photooxidation.

## Optical Setup

As the block diagram in Figure 1 shows, our measurements were performed using a continuous-wave (cw) 6-W argon-ion laser, a 2-W dye laser, a darkened 90° sample chamber, a 0.32-m monochromator, and a thermoelectrically cooled CCD array detector. The monochromator was IEEE-interfaced to a PC for data collection and analysis. All measurements were made at room temperature in air.

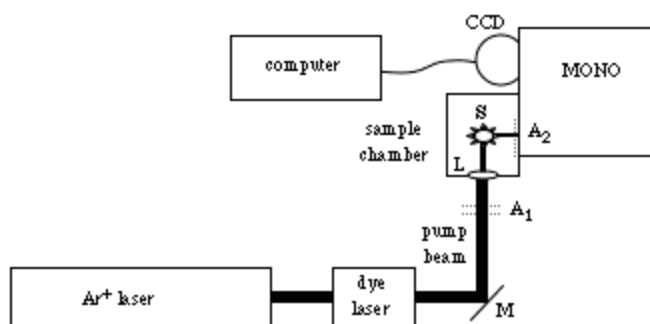


**Figure 1 .** The optical setup. The computer controls both the CCD detector and the monochromator (MONO). Other symbols used in the drawing: M = mirror, A<sub>1</sub> = attenuators before the sample, A<sub>2</sub> = attenuators at the entrance slit, L = lens, and S = sample.

The ion laser was used to pump the dye laser. The latter utilized rhodamine 6G perchlorate mixed in ethylene glycol, which gave us the ability to tune the pump wavelength over a range of 560 to 640 nm. Tuning was accomplished using a three-plate intracavity birefringent filter, spectrally calibrated against a standard Hg-Xe penlamp.

Initial alignment of the optics was performed using a multi-color helium-neon laser. This provides a simple method to excite samples for use in student laboratories in which a dye laser is not available or convenient, albeit at low powers and discrete wavelengths.

It is important to take precautions to avoid spurious effects in such a setup. The pump laser must strike the sample near the edge closest to the entrance slit to the monochromator. Otherwise the fluorescence may be reabsorbed or scattered by the parts of the sample between the pumped volume and the slit. The alignment of the sample and optics must not be disturbed during a run. The sample should be monitored for burning of physical holes at high pump intensities due to the thermal load from nonradiative de-excitations. This load can be estimated from the quantum yield (*i.e.*, the number of photons emitted per photon absorbed). As a baseline, the quantum yield for

cresyl violet in methanol solution is 0.54 (Magde 1979).

## Sample Preparation

We prepared both liquid and solid samples, beginning from powdered forms of the PMMA (also known as plexiglas, lucite, or acrylic) and dye (cf. Figure 2) and spectroscopic grade solvents. The liquid solutions were created by making an optically dense dye/ethanol mixture (about 0.2 mg/mL, 0.02% W/V, or  $6 \times 10^{-4}$  M), then passing it through a 0.45- $\mu$ m syringe filter to remove any undissolved particulates. A few milliliters of this solution was poured into a glass cuvette (transparent on four sides) and inserted in the sample chamber. Figure 3 is a photograph of one of the liquid solutions being excited by the dye laser.

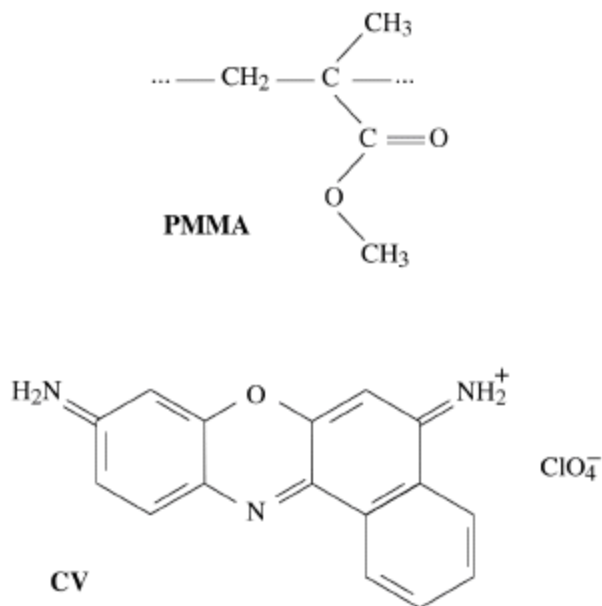


**Figure 2.** Chemical structure of the repeat unit of poly(methyl methacrylate), abbreviated PMMA, and of cresyl violet perchlorate (CV).

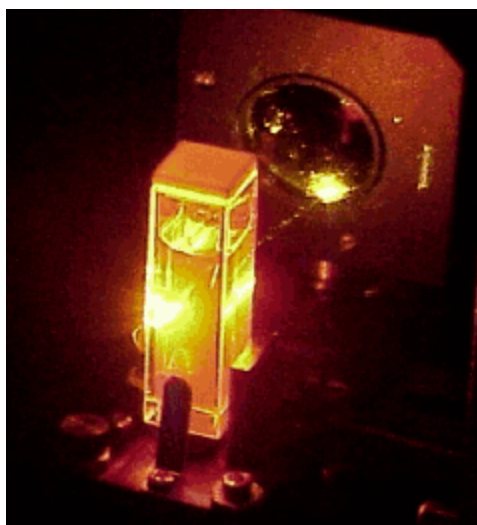


**Figure 3.** A liquid dye solution inside the sample chamber being excited by the pump beam entering through the lens from the rear. The excited spot is

near the left-hand edge of the cuvette, in the direction of the entrance slit (cf. Figure 1) off the left side of the picture.

The solid blocks were made using acetone as the solvent. High molecular weight polymer (*i.e.*, long, unbroken chains) improves the optical quality of the final samples. We used starting PMMA material with a weight of about one million. Approximately 10 g of polymer was dissolved in 25 mL of acetone in a wide-mouthed beaker to which about 1 g of dye was added. The beaker was left under a fume hood until all the acetone had evaporated (slowly so as to inhibit bubble formation), leaving a smooth piece of flat, colored plexiglas doped at 10 wt%. This was then cut into small pieces for spectral measurement. Pictured in Figure 4 are various dye-doped polymer samples. Each is about 1 cm<sup>2</sup> in area and about 1–2 mm thick.



**Figure 4.** A variety of pieces of PMMA doped with different laser dyes: styryl 9M, Rh6G, pyrromethene 567, and cresyl violet from left to right.

## Results

The curves in Figure 5 are the emission spectra of cresyl violet in PMMA. The fluorescence successively bleached away as energy was cycled through the sample. Notice that the decline is not uniform. Instead, it is roughly logarithmic in the pump energy. This incident energy was calculated as the amount of time that the dye was exposed to the exciting beam multiplied by the laser intensity, which was increased in discrete steps by removing neutral density filters in order to speed up the process. (These filters were moved from before to after the sample, at the locations shown in Figure 1, so as to maintain the signal level at the detector.) Figure 6 plots the detailed decrease in the peak signal with increasing time of exposure to the pump beam.

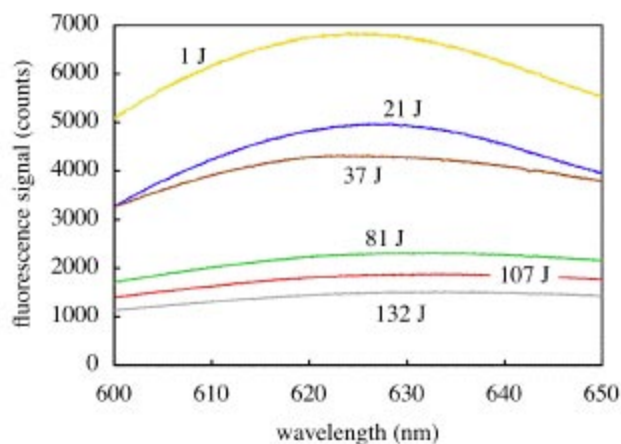


**Figure 5.** Fluorescence spectra of a cresyl-violet-doped PMMA sample that is bleaching with increasing total incident laser energy (as labeled on the curves).

The cuvettes of the dye in liquid solution showed minimal loss in fluorescence, even when high laser intensities were applied for long periods of time. This is due to the fact that the dye molecules are free to circulate and reorient within the cuvette. Because of this, the probability of exciting the same molecules repeatedly is greatly decreased and few molecules are bleached.

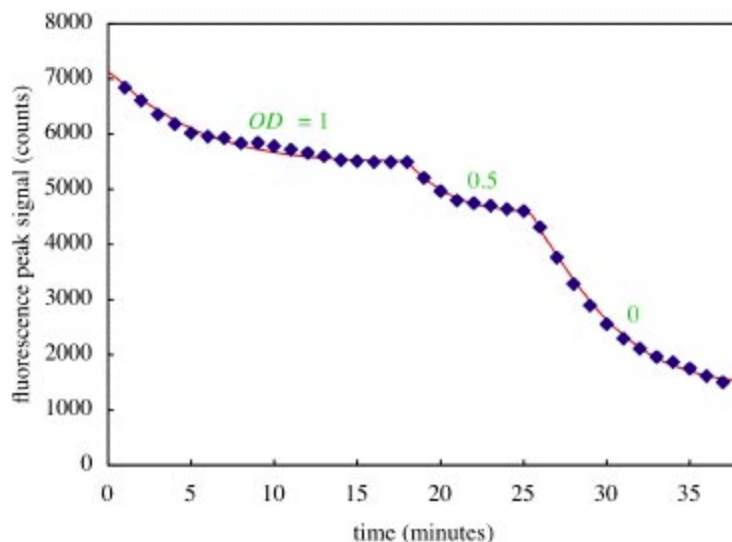


**Figure 6.** The decay in the fluorescence peak signal of CV:PMMA with pump exposure time. The blue diamonds are the background-corrected measured values, with error bars about the size of the plot symbols. The attenuators were changed at the two cusps, where the optical density (OD) in front of the sample is labeled in green. The red curve is a fit to Equation (8).

There is both a broadening and blue shifting of the unbleached fluorescence spectrum of cresyl violet in a solid sample of PMMA, compared to that of the same dye in ethanol solution. Specifically,  $\lambda_F = 625$  nm is the peak emission wavelength in the polymer, which is about 5 nm lower than in the liquid. This host dependence comes about because of the interactions of the dye molecules with its neighbors. Presumably the dye in the polymer can be “frozen” into strained configurations that alter the energy levels of the optically active  $\pi$ -orbital electrons.

## Theoretical Analysis and Discussion

The fluorescence power  $P_F$  (in W) is equal to the number density  $N_2$  (in  $\text{m}^{-3}$ ) of excited dye molecules multiplied by the product of the pumped volume of the sample  $\pi r^2 L$  (where  $r$  is the radius of the pump beam focal spot and  $L$  is the sample thickness) and the fluorescence photon energy  $hc / \lambda_F$  (where  $h$  is Planck’s constant and  $c$  is the speed of light) and divided by the excited state relaxation lifetime  $\tau$ , which is approximately 5.5 ns in both liquid and glassy ethanol (Narasimhan 1988) and is expected to be similar in our hosts. That is,

$$P_F = \frac{N_2 h c \pi r^2 L}{\lambda_F \tau} \quad (1)$$

The radius  $r$  of the focused pump spot was measured to be  $(165 \pm 25) \mu\text{m}$  by scanning a razor blade on a translational stage horizontally and vertically across the beam at the sample location.

The excitation intensity  $I_P = P_P / \pi r^2$  (where  $P_P = 145 \text{ mW} / 10^{OD}$  is the pump laser power with OD the optical density of the attenuators prior to the sample) is small compared to the saturation intensity  $I_S = h c / \lambda_P \sigma \tau$  (where  $\lambda_P = 585 \text{ nm}$  is the pump wavelength). Here the absorption cross

section at the pump wavelength is estimated to be  $\sigma = (1.0 \pm 0.1) \times 10^{-20} \text{ m}^2$  using the published extinction coefficient in ethanol (Drexhage 1990). Since  $I_P \ll I_S$ , stimulated emission can be neglected so that the rate of absorption must balance the spontaneous emission under steady state cw excitation,

$$N_2 = \frac{N}{1 + I_S / I_P} \cong \frac{I_P}{I_S} N \quad (2)$$

where  $N$  is the number density of unbleached dye molecules. This number can be related in turn to the transmittance of the sample,

$$T = \exp(-N \sigma L) \Rightarrow N = \frac{\ln(1/T)}{\sigma L} \quad (3)$$

neglecting the  $(n-1)^2 / (n+1)^2 = 4\%$  reflectance loss from each face (where the refractive index of plexiglas is  $n = 1.49$ ). Substituting Equation (3) into (2), and then that into (1) and simplifying leads to the compact result

$$\Phi_F = \Phi_P \ln(1/T) \quad (4)$$

where  $\Phi_F = P_F \lambda_F / h c$  and  $\Phi_P = P_P \lambda_P / h c$  are the fluorescence and pump photon fluxes (in photons/s), respectively.

The time-dependent transmittance of the sample as it bleaches during cw laser exposure is given by (Kaminow 1972)

$$T = \left[ 1 + (T_0^{-1} - 1) e^{-\beta t} \right]^{-1} \quad (5)$$

where  $T_0$  is the initial transmittance of the sample and the bleaching rate constant is

$\beta = \Phi_P \sigma / B \pi r^2$  with  $B$  the so-called bleaching number (*i.e.*, the average number of excitation-relaxation cycles a dye molecule undergoes before it bleaches). That is,  $B$  is the reciprocal of the bleaching quantum efficiency. Equation (5) assumes that the sample fully bleaches ( $T \rightarrow 1$ ) at long times ( $t \rightarrow \infty$ ). In contrast, at any fixed pump intensity, Figure 6 indicates that the

bleaching saturates at some lower transmittance  $T_\infty < 1$ , so that Equation (5) should be modified to

$$\frac{1}{T} = \frac{1}{T_\infty} + \left( \frac{1}{T_0} - \frac{1}{T_\infty} \right) e^{-\beta t} \quad (6)$$

This might arise from thermal effects (Fork 1972), stemming from the fraction of the incident light which heats the sample rather than being reradiated away, or from a site dependence of the photobleaching quantum efficiency (Higuchi 1983), assuming that the orientations or polymeric neighbors of the dye molecules strongly influence  $B$ .

Substituting Equation (6) into (4) and expressing  $T_0$  and  $T_\infty$  in terms of the corresponding fluorescence photon fluxes  $\Phi_{F0}$  and  $\Phi_{F\infty}$  using Equation (4) gives

$$\frac{\Phi_F - \Phi_{F\infty}}{\Phi_P} = \ln \left\{ 1 + \left[ \exp \left( \frac{\Phi_{F0} - \Phi_{F\infty}}{\Phi_P} \right) - 1 \right] e^{-\beta t} \right\} \quad (7)$$

However, the monochromator only collects a portion of the fluorescence. Using Equation (4) once more, one finally deduces

$$\frac{\Phi_F - \Phi_{F\infty}}{\Phi_{FU}} = \ln \left\{ 1 + \left[ \exp \left( \frac{\Phi_{F0} - \Phi_{F\infty}}{\Phi_{FU}} \ln \frac{1}{T_U} \right) - 1 \right] e^{-\beta t} \right\} / \ln \frac{1}{T_U} \quad (8)$$

where  $T_U$  and  $\Phi_{FU}$  are the transmittance and the fluorescence photon flux, respectively, of the unbleached sample. Since the fluorescence flux only appears as a ratio in Equation (8), the unknown geometrical factor representing the fraction of light collected drops out, and  $\Phi_F$  can be directly taken to be the number of CCD detector counts at  $\lambda_F = 625$  nm.

The unbleached transmittance of the sample was measured to be  $T_U = 1.6\%$  by exposing it to a low-intensity pump beam and calculating a ratio of the readings of a power meter placed before and after the sample. The unbleached peak fluorescence flux was deduced to be  $\Phi_{FU} = (7140 \pm 60)$  counts by extrapolating the signal in Figure 6 back to  $t = 0$ .

Equation (8) was then separately fit to each of the three pump intensities in Figure 6, restarting  $t$  at each knee (when an attenuator was moved). Note that  $\Phi_{F\infty}$  for one range of intensities becomes  $\Phi_{F0}$  in the successive range. This leaves two independent parameters for each data sequence, namely the bleached fluorescence flux  $\Phi_{F\infty}$  and the photooxidation rate constant  $\beta$ . The best-fit values are listed in Table 1. From these, we computed

$B = 10^{-OD} (1/\beta) (3.0 \pm 1.3) \times 10^6 / \text{min}$  after substituting the known values of the various parameters and constants. The bleaching number was found to vary from 1.1 to 8.4 million as the pump intensity was increased from 17 to 170 W/cm<sup>2</sup> (somewhat beyond the damage threshold of the sample, thus preventing us from continuing to yet higher laser powers). This compares favorably to 1.4 and 2.5 million measured for Rh6G in PMMA assuming isotropic and axial molecular geometries, respectively (Kaminow 1972). In liquid hosts, cresyl violet and rhodamine 6G have similar values for  $B$  (Beer 1972) and the present result suggests that the same is true of polymer hosts.

OD*	$\Phi_{F\infty}$ (counts) <sup>†</sup>	$1/\beta$ (min) <sup>‡</sup>	$B$ (millions) <sup>^</sup>	$f_{\text{bleach}}$ (%) <sup>**</sup>
1	5480±50	3.8±0.3	1.1±0.5	23±2
0.5	4530±70	2.3±0.6	2.2±1.2	37±2
0	1430±70	2.8±0.2	8.4±4.1	80±1

**Table 1 . Photobleaching of Cresyl Violet in PMMA**

\*Total optical density of the attenuators in front of the sample

†Fit value of  $\Phi_{F\infty}$

‡Fit value of  $1/\beta$

<sup>^</sup>Bleaching number calculated from  $\beta$

\*\*Total fraction of dye molecules in the pumped volume of the sample that has been oxidized at long exposures, as calculated using Equation (9)

Since  $\Phi_F \propto N$ , we can also calculate the cumulative fraction of dye molecules that have been bleached,

$$f_{\text{bleach}} = 1 - \frac{\Phi_{F\infty}}{\Phi_{FU}}. \quad (9)$$

As Table 1 indicates, about 80% of the cresyl violet molecules get photooxidized by the time the sample is experiencing substantial thermal damage. This correlation between dopant oxidation and host damage is probably not a coincidence, since both during and after bleaching the photoproducts may release chemical energy or absorb laser radiation and convert it into thermal energy.

## Conclusion

In conclusion, we have measured the quantum efficiency for photooxidation of cresyl violet in solid poly(methyl methacrylate). The key experimental data and theoretical fit are graphed in Figure 6, and the important parameters are summarized in Table 1.

Since the photooxidation irreversibly destroys the optical properties of the dye molecules, knowledge of this quantum efficiency is important in determining the lifetimes of the molecules in a given optical environment, and hence the possible technological applications of a given dye-host system. In particular, the photodegradation is minimal at low intensities, and thus this material can be used under ordinary brightness levels, such as in computer displays or electrical indicator lamps. On the other hand, this dye-doped plastic would have severely limited longevity in laser amplifiers, detectors, optical fibers, and other applications in which high intensities are required.

Other variables not investigated in this study that may affect photostability of the dye molecules include temperature of the sample, nature of the polymer, and degree of alignment of the long-chained polymer molecules. Further research into these issues could open up or rule out other possible applications of dye-doped organic materials.

## Acknowledgements

We thank the Research Corporation and the Office of Naval Research for their generous support.

---

## References

- Beer, D and J Weber. (1972). Photobleaching of organic laser dyes. *Optics Communications*. 5: 307–309.
- Castelli, F. (1975). Stimulated emission of cresyl violet pumped by N<sub>2</sub> laser or rhodamine 6G dye laser. *Applied Physics Letters*. 26: 18–19.
- Drexhage, KH. (1990). Structure and properties of laser dyes. In FP Schäfer (Ed.), *Dye Lasers*, 3rd ed. Berlin, Springer-Verlag, 155–200.
- Fork, RL and Z Kaplan. (1972). Increased resistance to photodegradation of rhodamine 6G in cooled solid matrices. *Applied Physics Letters*. 20: 472–474.
- Higuchi, F and J Muto. (1983). On the photobleaching quantum yields of heat-treated rhodamine 6G (Rh6G) molecules in the copolymer of methyl methacrylate (MMA) with methacrylic acid (MA). *Physics Letters*. 99A: 121–124.
- Kaminow, IP et al. (1972). Photobleaching of organic laser dyes in solid matrices. *Applied Optics*. 11: 1563–1567.
- Mackey, MS and WN Sisk. (2001). Photostability of pyrromethene 567 laser dye solutions via photoluminescence measurements. *Dyes and Pigments*. 51: 79–85.
- Magde, D et al. (1979). Absolute luminescence yield of cresyl violet: A standard for the red. *Journal of Physical Chemistry*. 83: 696–699.



Moore, CA and CD Decker. (1978). Power-scaling effects in dye lasers under high-power laser excitation. *Journal of Applied Physics*. 49: 47–60.

Narasimhan, LR et al. (1988). Solute-solvent dynamics and interactions in glassy media: Photon echo and optical hole burning studies of cresyl violet in ethanol glass. *Chemical Physics Letters*. 152: 287–293.

Schäfer, FP. (1992). Dye lasers and laser dyes in physical chemistry. In M Stuke (Ed.), *Dye Lasers: 25 Years*. Berlin, Springer-Verlag, 19–36.

Journal of Young Investigators. 2004. Volume Ten.  
Copyright © 2004 by Michael J. Holmes, 2nd Lt., USMC and JYI. All rights reserved.

JYI is supported by: The National Science Foundation, The Burroughs Wellcome Fund, Glaxo Wellcome Inc., Science Magazine, Science's Next Wave, Swarthmore College, Duke University, Georgetown University, and many others.

Copyright ©1998-2004 The Journal of Young Investigators, Inc.